



## Article

# Sorption and Desorption of Vanadate, Arsenate and Chromate by Two Volcanic Soils of Equatorial Africa

Sara Gonzalez-Rodriguez<sup>1</sup> and Maria Luisa Fernandez-Marcos<sup>1,2,\*</sup>

<sup>1</sup> Department of Soil Science and Agricultural Chemistry, Universidad de Santiago de Compostela, 27002 Lugo, Spain; sara.gonzalez@inclusion.gob.es

<sup>2</sup> Institute of Agricultural Biodiversity and Rural Development, University of Santiago de Compostela, 27002 Lugo, Spain

\* Correspondence: mluisa.fernandez@usc.es

**Abstract:** Sorption of oxyanions by soils and mineral surfaces is of interest due to their role as nutrients or pollutants. Volcanic soils are variable charge soils, rich in active forms of aluminum and iron, and capable of sorbing anions. Sorption and desorption of vanadate, arsenate, and chromate by two African andosols was studied in laboratory experiments. Sorption isotherms were determined by equilibrating at 293 K soil samples with oxyanion solutions of concentrations between 0 and 100 mg L<sup>-1</sup> V, As, or Cr, equivalent to 0–2.0 mmol V L<sup>-1</sup>, 0–1.3 mmol As L<sup>-1</sup>, and 0–1.9 mmol Cr L<sup>-1</sup>, in NaNO<sub>3</sub>; V, As, or Cr were determined by ICP-mass spectrometry in the equilibrium solution. After sorption, the soil samples were equilibrated with 0.02 M NaNO<sub>3</sub> to study desorption. The isotherms were adjusted to mathematical models. After desorption with NaNO<sub>3</sub>, desorption experiments were carried out with a 1 mM phosphate. The sorption of vanadate and arsenate was greater than 90% of the amount added, while the chromate sorption was much lower (19–97%). The sorption by the Silandic Andosol is attributed to non-crystalline Fe and Al, while in the Vitric Andosol, crystalline iron species play a relevant role. The V and Cr sorption isotherms fitted to the Freundlich model, while the As sorption isotherms conformed to the Temkin model. For the highest concentrations of oxyanions in the equilibrating solution, the sorbed concentrations were 37–38 mmol V kg<sup>-1</sup>, 25 mmol As kg<sup>-1</sup>, and 7.2–8.8 mmol Cr kg<sup>-1</sup>. The desorption was low for V and As and high for Cr. The comparison of the sorption and desorption isotherms reveals a pronounced hysteresis for V in both andosols and for Cr in the Silandic Andosol. Phosphate induced almost no V desorption, moderate As desorption, and considerable Cr desorption.



**Citation:** Gonzalez-Rodriguez, S.; Fernandez-Marcos, M.L. Sorption and Desorption of Vanadate, Arsenate and Chromate by Two Volcanic Soils of Equatorial Africa. *Soil Syst.* **2021**, *5*, 22. <https://doi.org/10.3390/soilsystems5020022>

Academic Editor: Evert Elzinga

Received: 1 January 2021

Accepted: 15 March 2021

Published: 1 April 2021

**Publisher's Note:** MDPI stays neutral with regard to jurisdictional claims in published maps and institutional affiliations.



**Copyright:** © 2021 by the authors. Licensee MDPI, Basel, Switzerland. This article is an open access article distributed under the terms and conditions of the Creative Commons Attribution (CC BY) license (<https://creativecommons.org/licenses/by/4.0/>).

**Keywords:** andosol; Silandic Andosol; Vitric Andosol; andosols; oxyanions; potentially toxic elements; Rwanda; São Tomé and Príncipe; Freundlich isotherm; Temkin isotherm

## 1. Introduction

Sorption of oxyanions by soils and mineral surfaces has received considerable attention [1–10] because of their important role as nutrients or pollutants. Sorption refers to the retention of molecules or ions by active surfaces and encompasses adsorption, surface precipitation, and polymerization [11]. The presence of reactive aluminum and iron phases, such as oxides, hydroxides, oxyhydroxides, poorly crystalline aluminosilicates (allophane, imogolite), or Al (Fe)-humus complexes, endows soils with variable charge and anion retention capacity. Anions can be adsorbed onto reactive surfaces by chemical bonding (chemisorption or specific adsorption), leading to the formation of inner-sphere complexes, or by physical forces (physical adsorption), which leads to the formation of outer-sphere complexes [11,12].

Vanadium (V) is a trace metal relatively abundant in the Earth's crust, with an average concentration of 97 mg kg<sup>-1</sup> in the upper continental crust [13], being more concentrated in mafic than in acidic rocks. However, the anthropogenic emissions of V to the environment

currently exceed the natural sources, according to Schlesinger et al. [13]. The major anthropogenic sources of V are mining, steel industry, fertilizers, pesticides, waste, and, especially, combustion of fossil fuels [14]. Vanadium emissions to the environment are increasing worldwide [15], resulting in increasing concentrations in waters, soils, and sediments. High concentrations of V can be toxic to humans and other organisms [13,16–22] and it is listed in the USEPA Contaminant Candidate List 4 [23]. The most stable oxidation state of vanadium in aerobic environments is +5, which usually occurs as vanadate ( $\text{H}_2\text{VO}_4^-$ ,  $\text{HVO}_4^{2-}$ ) and is the most mobile and toxic form of vanadium [16,21]. Vanadate is strongly adsorbed onto poorly crystalline (oxyhydr)oxides [24,25], particularly at low pH. According to Larsson et al. [18,26], V toxicity to plants and soil microorganisms is controlled by the vanadium sorption capacity of soils. Adsorption of both V(IV) and V(V) by metal (oxyhydr)oxides occurs mainly through the formation of inner-sphere complexes [22,27]. Vanadate competes with other oxyanions for sorption sites on positively charged mineral surfaces, being bound even more strongly than phosphate and arsenate on Fe hydrous oxides [16,28,29].

Arsenic (As) is a ubiquitous element, with an average concentration of  $1.8 \text{ mg kg}^{-1}$  in the Earth's crust, and is part of numerous minerals including arsenates, arsenites, arsenides, and sulfides [12,17,30]. It is highly toxic for humans, animals, and plants, and its toxicity has been known from ancient times. Humans are exposed to arsenic mainly through the air, food, and water [31]. The ingestion of arsenic can result in both cancer (skin, lung, and bladder) and non-cancer effects (skin lesions) [30]. Contamination of groundwater by arsenic is a serious threat to humanity worldwide. The presence of As in the environment may arise from natural sources or anthropogenic activities [17,30]. Anthropogenic sources of As include mining, past use of arsenical pesticides, coal combustion, and waste disposal. The dominant forms of arsenic in soils are arsenate [As(V)] and arsenite [As(III)] [17,30], with arsenate ( $\text{H}_2\text{AsO}_4^-$ ,  $\text{HAsO}_4^{2-}$ ) predominating in well-aerated media. Among oxyanion-forming elements, arsenic is one of those that pose a greater environmental risk, due to its mobility over a wide range of redox conditions [30]. Arsenite is more toxic and mobile than arsenate [12,30]. The As mobility and availability in soils is controlled by sorption onto soil components, especially variable charge materials (Fe, Al, and Mn (oxyhydr)oxides, allophane, imogolite), and complexation by soil organic matter [12,30,32]. Arsenates and arsenites are sorbed onto soil components through the formation of inner-sphere complexes [12,30].

Chromium (Cr) is a relatively abundant element in the Earth's crust, where its average concentration is  $100 \text{ mg kg}^{-1}$  [17]. Its concentration is higher in mafic and ultramafic rocks and in soils derived from them. The presence of chromium in soils is, to a large extent, lithogenic [25,33,34]. In addition to a lithological origin, chromium in the environment can be related to various human activities (mining, smelting industry, fuel combustion, electroplating, leather tanning, waste disposal, and soil organic amendments) [17,35,36]. It can occur in soils in the oxidation states +3 and +6, Cr(VI) being more mobile and toxic than Cr(III) [37]. Readily soluble Cr(VI) in soils is toxic to plants and animals, being a known carcinogenic agent [38]. High concentrations of Cr in soils pose an environmental risk, particularly in soils for agricultural use. The high toxicity and mobility of chromium make its sorption by soil an issue of paramount importance. In acid soils, Cr(VI) is removed from soil solution by adsorption on positively charged sorption sites [36]. Chromate ( $\text{HCrO}_4^-$ ,  $\text{CrO}_4^{2-}$ ) sorption by variable charge soils occurs through both specific (inner-sphere) adsorption and electrostatic (outer-sphere) adsorption [39,40].

The adsorption of oxyanions by natural components determines their mobility, availability, and toxicity [11,41]. The sorption of vanadate, arsenate, or chromate by soils is a decontaminating process that protects waters and vegetation from pollution by these species.

Volcanic soils cover 1% of the Earth's surface and support 10% of the world's population [42]. They are variable-charge soils, rich in active forms of aluminum and iron, and capable of adsorbing phosphate and other anions [43].

Although much work has been devoted to the study of oxyanions sorption by individual minerals, relatively few studies address oxyanions sorption by soils, and very little information exists on oxyanions sorption and desorption by African soils.

Rwanda is part of a large metallogenic province in Central Africa [44]. Mining is an important economic activity in Rwanda, comprising mining of tin, niobium, tantalum, tungsten, and gold. Presently, mining activity is mainly artisanal, with some semi-industrial, small-scale mining. Many historic mining sites have been abandoned without remediation, leaving behind waste dumps and degraded landscapes [45]. Residues from mining activity and mineral processing are released into the environment. Often, in the vicinity of mining sites, farming activities take place, which are affected by potentially toxic elements (PTE) from mining, with the consequent effects on the quality of food products and on human health [45]. Hilly relief and high slopes along with deforestation promote runoff and subsequent pollution of water courses.

Tungsten ores from Rwanda were reported to be rich in vanadium and arsenic [46]. Arsenopyrite commonly occurs in tin deposits, being a source of As [47]. Volcanic rocks of Rwanda are reported to have elevated concentrations of vanadium and chromium [48,49]. High concentrations of arsenic were found in tailings, stream sediments, soils, and water samples close to mining sites in Rwanda [45,50]. In this country, volcanic soils occupy nearly 3% of the land surface and are crucial for population livelihoods.

São Tomé is a small volcanic island of the Republic of São Tomé and Príncipe, belonging to the volcanic alignment known as the “Cameroon Hot Line”. Excepting soils developed from alluvial deposits, most São Tomé soils derive from volcanic materials. Basaltic rocks on São Tomé Island are often rich in chromium and vanadium [51,52].

PTE immobilization by soil sorption is of paramount importance to preserve environmental quality and human health.

The present paper aims to study the sorption and desorption of vanadate, arsenate, and chromate by the surface horizons of two soils representative of volcanic areas in Equatorial Africa: a Silandic Andosol [53] on volcanic ash (Rwanda) and a Vitric Andosol on basaltic material (São Tomé and Príncipe). Silandic Andosols are characterized by their richness in short-range-order silicates (allophane, imogolite), while Vitric Andosols are characterized by the presence of volcanic glass and a lower content of short-range-order minerals (lesser degree of weathering). Both non-crystalline and crystalline iron and aluminum forms are reported to adsorb oxyanions [1,3,5,6,22,26,28,29,40,41,54–58]. The sorption and desorption will be adjusted to common mathematical models and the role of phosphate in the desorption will be addressed.

## 2. Materials and Methods

### 2.1. Soils

The soils used in the study were the surface horizons (0–20 cm) of two agricultural soils from Rwanda and São Tomé and Príncipe. The Rwanda soil, developed from volcanic ash, is classified as Silandic Andosol [53], while the soil of São Tomé Island (São Tomé and Príncipe) classifies as Vitric Andosol. Figure 1 and Table 1 show the geographical location and some relevant properties of the two soils studied. The acid oxalate extraction estimates active forms of aluminum and iron. Oxalate-extractable aluminum ( $Al_o$ ) consists mainly of aluminum in organic complexes, in non-crystalline hydrated oxides, in allophane, and imogolite [59,60], while oxalate-extractable iron ( $Fe_o$ ) is mainly constituted by ferrihydrite [43,60]. The concentrations of aluminum and iron extractable by acid oxalate fulfil the requirement for andic properties ( $Al_o + 1/2 Fe_o > 2\%$ ) [53] in the soil of Rwanda and for vitric properties ( $0.4\% < Al_o + 1/2 Fe_o < 2\%$ ) in the soil of São Tomé.



**Figure 1.** Location of the Vitric Andosol (São Tomé) and the Silandic Andosol (Rwanda).

The extraction by dithionite-citrate estimates the total free iron ( $Fe_d$ ), including non-crystalline forms of iron ( $Fe_o$ ) and crystalline oxyhydroxides (goethite, hematite, magnetite) [59,60], while the aluminum extracted by dithionite-citrate ( $Al_d$ ) includes non-crystalline aluminum forms (excepting non-crystalline aluminosilicates) and aluminum occluded in crystalline iron oxyhydroxides [59]. According to Sanchez et al. [61], São Tomé's Vitric Andosol has a high  $Fe_d$  concentration (7.84%), resulting in high P fixation capacity. This soil presents moderate concentrations of non-crystalline Fe and Al, but a large content of crystalline iron oxyhydroxides (Table 1). Conversely, the Rwandan Silandic Andosol has a  $Fe_o/Fe_d$  ratio of 0.75, which indicates the predominance of non-crystalline over crystalline iron forms. The higher  $Al_d$  compared to  $Al_o$  in the São Tomé Vitric Andosol indicates the presence of aluminum in the crystalline lattices of iron oxyhydroxides.

**Table 1.** Location, pH, organic carbon, texture, available P, aluminum, and iron extracted by acid oxalate and by dithionite-citrate and pH in NaF of the studied soils.

Soil	Location	Altitude, m	pH	C, %	Texture	Mehlich-3 P, $mg\ kg^{-1}$	%				
							$Fe_o$	$Al_o$	$Fe_d$	$Al_d$	$pH_{NaF}$
Silandic Andosol	01°36'32" S, 29°32'57" E	311	5.60	6.18	Sandy loam	32.2	3.46	2.48	4.60	1.81	11.07
Vitric Andosol	00°20'00" N, 06°39'00" E	2368	6.30	7.46	Silty loam	13.5	1.11	0.40	7.84	1.74	8.39

$Fe_o$ ,  $Al_o$ : Fe and Al extracted by acid ammonium oxalate [62];  $Fe_d$ ,  $Al_d$ : Fe and Al extracted by dithionite-citrate [63].

Values of pH in NaF higher than 9.5 indicate the presence of allophane and/or organo-aluminum complexes [53], materials active in the fixation of anions.

Both soils showed high and hardly reversible phosphate sorption, somewhat higher in the Silandic Andosol [64]. The phosphate sorption isotherms conformed to the Temkin model. The soil samples were air-dried and sieved (<2 mm) prior to analysis.

## 2.2. Sorption and Desorption Isotherms

The sorption isotherms were determined in batch experiments, equilibrating 0.5 g soil, weighed with a precision of a ten-thousandth of a gram, with 10 mL of solution of vanadate, arsenate, or chromate in 0.02 M NaNO<sub>3</sub> as background electrolyte at room temperature (293 K). The oxyanion concentrations in the equilibrating solutions ranged between 0 and 100 mg·L<sup>-1</sup> (0, 2, 4, 10, 20, 40, 60, and 100 mg L<sup>-1</sup>) of the element (V, As, or Cr), equivalent to 0–2.0 mmol V L<sup>-1</sup>, 0–1.3 mmol As L<sup>-1</sup>, and 0–1.9 mmol Cr L<sup>-1</sup>, and the solution pH was adjusted to the value of soil pH. The concentration range was chosen to approach the sorption capacity, after preliminary tests with shorter ranges revealed that most of the added anions were sorbed by the soil. The suspensions were shaken for 24 h, centrifuged at 6000 rpm for 15 min, and filtered through acid-washed filter paper. The determinations were carried out in triplicates. Soil pH was determined in the equilibrium solutions using a CRISON pH-meter with a combined glass electrode. V, As, or Cr were determined in the equilibrium solutions by ICP-mass spectrometry in Varian 820-NS equipment. The sorbed anions were calculated as the difference between added V, As, or Cr and V, As, or Cr in the equilibrium solution.

Desorption experiments were carried out in soil samples previously equilibrated with various oxyanion concentrations. After removing the supernatant solution, 10 mL of 0.02 M NaNO<sub>3</sub> solution adjusted to the soil pH were added, the suspensions shaken for 24 h, centrifuged at 6000 rpm for 15 min, and filtered through acid-washed filter paper. pH and V, As, or Cr were determined in the equilibrium solution in the same way as in the sorption experiments. The anion concentration remaining in the sorbed phase was calculated from the concentration sorbed after the sorption equilibrium and the concentration released to the solution, making a correction to take into account the solution embedded in the solid after the sorption equilibrium. After desorption with dilute NaNO<sub>3</sub>, desorption experiments were carried out with a 1 mM solution of 50:50 KH<sub>2</sub>PO<sub>4</sub>:K<sub>2</sub>HPO<sub>4</sub>, to promote desorption using a competitor anion [65].

Sorption and desorption isotherms were obtained by plotting the anion concentration in the sorbed phase versus the solution concentration at equilibrium. The isotherms were fitted to mathematical models, namely the Langmuir, Freundlich, and Temkin isotherms [66].

The Langmuir isotherm is depicted by the equation  $Q = Q_{\max} * K_L * c / (1 + K_L * c)$ , where  $Q$  is the concentration of the adsorbed anion (mmol kg<sup>-1</sup>),  $c$  is the concentration in the liquid phase at equilibrium (μmol L<sup>-1</sup>),  $K_L$  is a constant related to the adsorption energy, and  $Q_{\max}$  (mmol kg<sup>-1</sup>) is the maximum adsorption capacity. The Langmuir model assumes that adsorption is restricted to a monolayer, that all the adsorption sites have the same adsorption energy, and that there is no interaction among the adsorbed molecules (or ions) [67].

The Freundlich isotherm is described by the equation  $Q = K_F * c^m$ , where  $Q$  and  $c$  have the same meaning as in the Langmuir equation,  $K_F$  is the adsorption constant, and  $m$  is a constant whose value varies between 0 and 1. The Freundlich model assumes that the adsorption surface is heterogeneous, and that the adsorption energy decreases exponentially as the concentration in the adsorbed phase increases. It does not predict an adsorption maximum [67].

The Temkin isotherm is described by the equation  $Q = (RT/b) * \ln(Ac)$  or  $Q = B * \ln(Ac)$ , where  $Q$  and  $c$  have the same meaning as in the Langmuir equation,  $R$  is the ideal gas constant (8.314 J mol<sup>-1</sup> K<sup>-1</sup>),  $T$  is the absolute temperature (in our case 293 K, that is 20 °C) and  $A$  and  $b$  are constants related to the heat of adsorption. It considers that the adsorption surface is heterogeneous, and that the adsorption energy decreases linearly with the concentration in the adsorbed phase. There is no maximum adsorption [67].

## 3. Results

In both sorption and desorption experiments, the pH values in the equilibrating solution and in the equilibrium solutions did not show significant differences.



### 3.1. Vanadate

Both studied soils showed a very high sorption of vanadate (Table 2), which approached 100% for an added concentration up to 20 mg V L<sup>-1</sup> (0.39 mmol L<sup>-1</sup>). For the highest concentration (100 mg V L<sup>-1</sup> or 2.0 mmol L<sup>-1</sup>), the sorption was 97% in the Silandic Andosol (Rwanda) and 96% in the Vitric Andosol (São Tomé). The sorbed V reached 38 mmol V kg<sup>-1</sup> in the Silandic Andosol (Rwanda) and 37 mmol V kg<sup>-1</sup> in the Vitric Andosol (São Tomé) for a V concentration of 2.0 mmol L<sup>-1</sup> (100 mg L<sup>-1</sup>) in the equilibrating solution.

**Table 2.** Percent sorption and desorption of oxyanions in the studied soils.

V in the equilibrating solution, mg L <sup>-1</sup>	Vitric Andosol			Silandic Andosol		
	% V sorption	% V desorption with NaNO <sub>3</sub>	% additional V desorption with phosphate	% V sorption	% V desorption with NaNO <sub>3</sub>	% additional V desorption with phosphate
2	99.8 ± 0.0	0.35 ± 0.15	0.15 ± 0.02	99.9 ± 0.0	0.32 ± 0.05	0.14 ± 0.01
4	99.9 ± 0.0	0.11 ± 0.07	0.06 ± 0.00	99.9 ± 0.0	0.14 ± 0.00	0.10 ± 0.00
10	99.9 ± 0.0	0.06 ± 0.01	0.06 ± 0.01	99.9 ± 0.0	0.11 ± 0.01	0.09 ± 0.01
20	99.7 ± 0.1	0.33 ± 0.03	0.18 ± 0.02	99.4 ± 0.1	0.38 ± 0.07	0.25 ± 0.03
40	98.5 ± 0.4	0.68 ± 0.03	0.27 ± 0.09	98.3 ± 0.6	0.67 ± 0.07	0.47 ± 0.06
60	98.2 ± 0.7	1.42 ± 0.16	0.25 ± 0.05	97.3 ± 0.4	1.24 ± 0.18	0.50 ± 0.07
100	95.7 ± 0.4	3.13 ± 0.02	0.24 ± 0.11	97.3 ± 0.5	2.71 ± 0.18	0.47 ± 0.04
As in the equilibrating solution, mg L <sup>-1</sup>	% As sorption	% As desorption with NaNO <sub>3</sub>	% additional As desorption with phosphate	% As sorption	% As desorption in NaNO <sub>3</sub>	% additional As desorption with phosphate
2	99.9 ± 0.1	0.00 ± 0.00	5.89 ± 0.01	99.8 ± 0.1	0.04 ± 0.03	7.25 ± 0.70
4	99.8 ± 0.1	0.06 ± 0.01	7.55 ± 0.58	99.7 ± 0.1	0.12 ± 0.03	9.26 ± 0.40
10	99.8 ± 0.0	0.08 ± 0.05	8.64 ± 0.54	99.6 ± 0.1	0.20 ± 0.10	9.86 ± 1.36
20	99.8 ± 0.2	0.10 ± 0.05	8.77 ± 0.31	99.7 ± 0.1	0.65 ± 0.10	11.1 ± 0.6
40	99.5 ± 0.2	0.33 ± 0.04	11.8 ± 0.26	98.9 ± 0.1	1.97 ± 0.03	28.7 ± 2.1
60	99.6 ± 0.1	0.89 ± 0.10	13.3 ± 0.74	97.4 ± 0.4	1.87 ± 0.32	33.3 ± 2.6
100	99.1 ± 0.7	2.21 ± 0.16	14.0 ± 1.32	94.8 ± 1.8	4.93 ± 0.57	33.9 ± 3.6
Cr in the equilibrating solution, mg L <sup>-1</sup>	% Cr sorption	% Cr desorption with NaNO <sub>3</sub>	% additional Cr desorption with phosphate	% Cr sorption	% Cr desorption in NaNO <sub>3</sub>	% additional Cr desorption with phosphate
2	97.1 ± 0.2	2.2 ± 0.1	2.1 ± 0.4	56.2 ± 1.6	34.7 ± 1.0	24.0 ± 1.6
4	94.1 ± 2.1	2.1 ± 0.2	2.5 ± 0.2	53.0 ± 0.7	30.1 ± 3.6	21.1 ± 4.3
10	95.9 ± 0.6	2.3 ± 0.1	2.2 ± 0.3	42.7 ± 3.2	37.8 ± 3.7	27.0 ± 0.9
20	46.9 ± 5.8	29.6 ± 2.8	16.6 ± 2.2	38.3 ± 2.4	36.9 ± 3.4	24.7 ± 2.1
40	35.6 ± 5.4	31.6 ± 3.7	18.5 ± 1.0	39.9 ± 4.1	33.4 ± 1.3	18.2 ± 0.5
60	28.8 ± 3.1	30.8 ± 2.2	18.2 ± 3.6	34.8 ± 5.5	30.3 ± 3.8	15.9 ± 3.1
100	19.0 ± 2.1	37.7 ± 7.6	20.2 ± 4.0	23.2 ± 1.2	30.9 ± 2.9	21.6 ± 1.1

The sorption isotherms (Figure 2) showed very similar vanadium sorptions by the Vitric and Silandic Andosols.

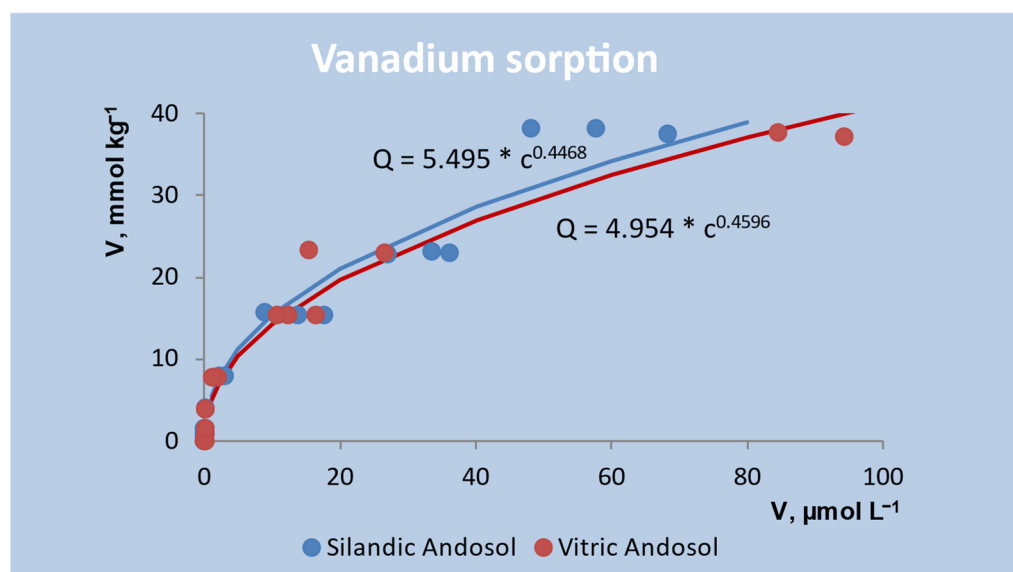


**Figure 2.** V sorption isotherms (sorbed V ( $\text{mmol kg}^{-1}$ ) vs. V concentration in the equilibrium solution ( $\mu\text{mol L}^{-1}$ )) fitted to the Freundlich model.

The sorption data were adjusted to the Langmuir, Freundlich, and Temkin models to find the best fit. Sorption for both soils fitted better the Freundlich model ( $r^2 = 0.911$  for the Vitric Andosol and  $0.957$  for the Silandic Andosol). The fitted equations were  $Q = 4.954 * c^{0.4596}$  for the Vitric Andosol and  $Q = 5.495 * c^{0.4468}$  for the Silandic Andosol. The constant  $K_F$  was slightly higher in the Silandic Andosol (5.495 vs. 4.954), while the constant  $m$  was very similar in both soils (0.4596 and 0.4468).

The V desorption in  $\text{NaNO}_3$  was always less than 4% of the V sorbed in both soils (Table 2). The desorption isotherms (Figure 3) also fitted the Freundlich model. The fitted equations were  $Q = 5.528 * c^{0.5047}$ ,  $r^2 = 0.861$  for the Vitric Andosol and  $Q = 5.198 * c^{0.5680}$ ,  $r^2 = 0.915$  for the Silandic Andosol.

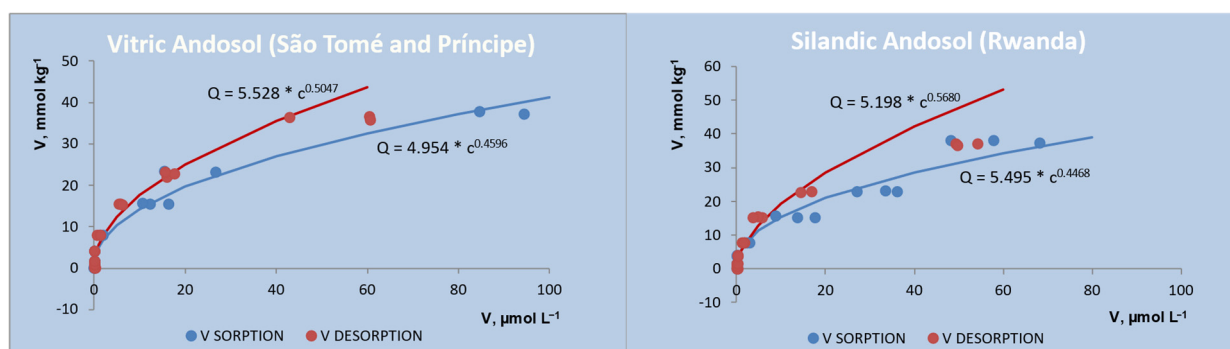


**Figure 3.** V sorption and desorption isotherms (sorbed V ( $\text{mmol kg}^{-1}$ ) vs. V concentration in the equilibrium solution ( $\mu\text{mol L}^{-1}$ )) fitted to the Freundlich model.

The addition of phosphate resulted in a little additional desorption of vanadate, the total desorption never attaining 4% (Table 2).

### 3.2. Arsenate

The arsenic sorption by both soils was extremely high, approaching 100% of the amount added for initial concentrations of up to  $40 \text{ mg L}^{-1}$  ( $0.53 \text{ mmol L}^{-1}$ ) in the Silandic Andosol and for the entire interval studied in the Vitric Andosol (Table 2). Unlike vanadate, the arsenate sorption was higher in the Vitric Andosol than in the Silandic

Andosol (Figure 4). The sorbed As reached 25 mmol As kg<sup>-1</sup> in both andosols for an As concentration of 1.3 mmol L<sup>-1</sup> (100 mg L<sup>-1</sup>) in the equilibrating solution.

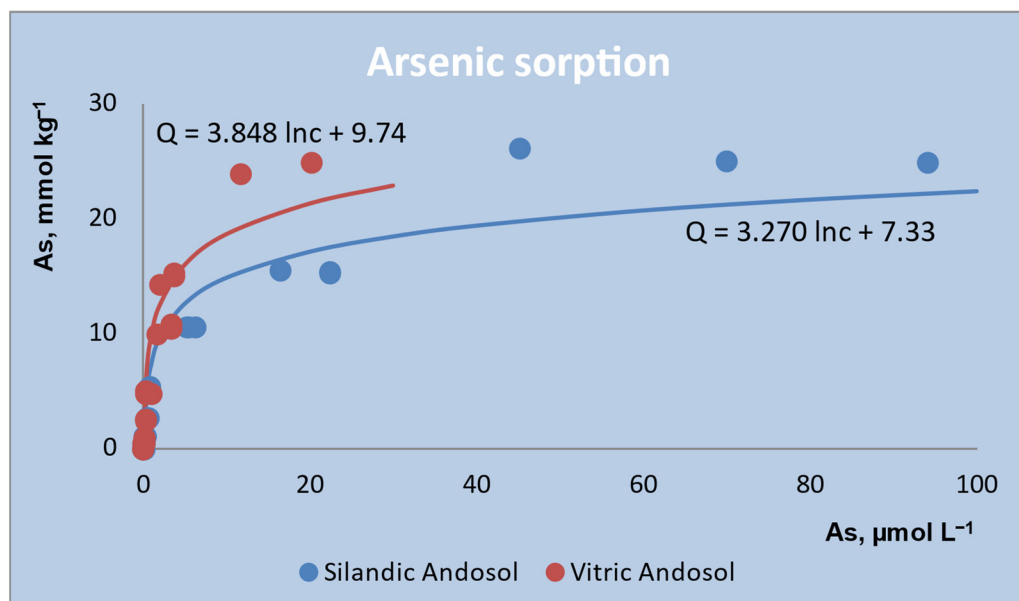


**Figure 4.** As sorption isotherms (sorbed As (mmol kg<sup>-1</sup>) vs. As concentration in the equilibrium solution (μmol L<sup>-1</sup>)) fitted to the Temkin model.

The sorption fitted the Temkin isotherm in both soils ( $r^2 = 0.886$  for the Vitric Andosol and  $0.906$  for the Silandic Andosol). The fitted equations were  $Q = 3.848 \ln c + 9.74$  for the Vitric Andosol and  $Q = 3.270 \ln c + 7.33$  for the Silandic Andosol. The constants A and B were higher in the Vitric Andosol than in the Silandic Andosol (A is 12.56 in the Vitric Andosol vs. 9.42 in the Silandic Andosol; B is 3.848 in the Vitric Andosol vs. 3.270 in the Silandic Andosol).

The As desorption in NaNO<sub>3</sub> was less than 5% of the As sorbed in both soils, being somewhat lower in the Vitric Andosol (Table 2). The desorption isotherms (Figure 5) also fitted the Temkin model. The fitted equations were  $Q = 2.939 \ln c + 10.60$ ,  $r^2 = 0.834$  for the Vitric Andosol and  $Q = 2.128 \ln c + 8.78$ ,  $r^2 = 0.808$  for the Silandic Andosol. The sorption and desorption isotherms were almost coincident (Figure 5), indicating the reversibility of the process.

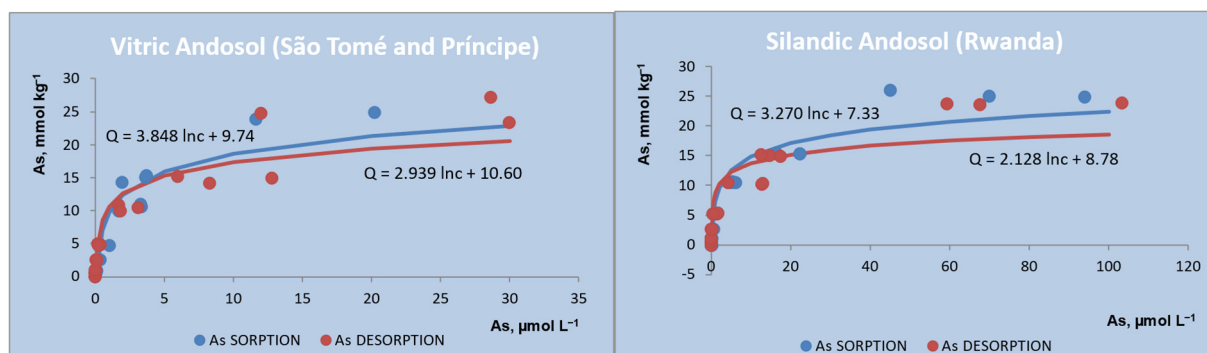


**Figure 5.** As sorption and desorption isotherms (sorbed As (mmol kg<sup>-1</sup>) vs. As concentration in the equilibrium solution (μmol L<sup>-1</sup>)) fitted to the Temkin model.

The addition of phosphate caused a considerably higher desorption than that obtained in NaNO<sub>3</sub> (Table 2), the additional desorption exceeding 30% of the absorbed As for the highest phosphate addition in the Silandic Andosol (Rwanda). Similar to the desorption



with  $\text{NaNO}_3$ , the amount of As desorbed by phosphate was higher in the Silandic Andosol, showing the strong retention of As by the Vitric Andosol.

### 3.3. Chromate

The chromate sorption was relatively low (between 19 and 97% of the added amount in the Vitric Andosol and between 23 and 56% in Silandic Andosol, Table 2). The sorbed Cr reached  $8.8 \text{ mmol Cr kg}^{-1}$  in the Silandic Andosol (Rwanda) and  $7.2 \text{ mmol Cr kg}^{-1}$  in the Vitric Andosol (São Tomé) for a Cr concentration of  $1.9 \text{ mmol L}^{-1}$  ( $100 \text{ mg L}^{-1}$ ) in the equilibrating solution. Chromate was more sorbed by the Vitric Andosol in the low concentration range, while at high concentrations, it was the Silandic Andosol that sorbed more (Figure 6).

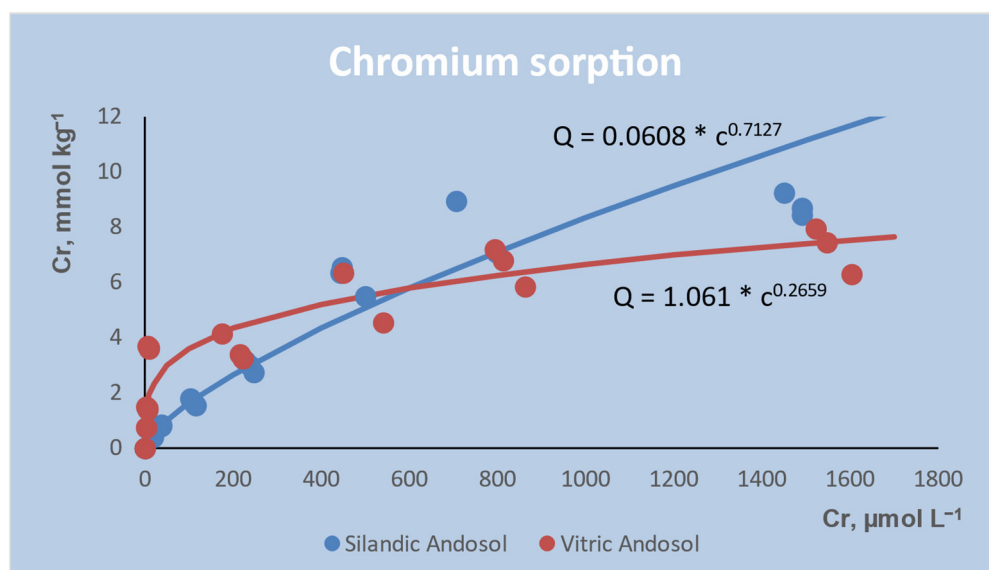


**Figure 6.** Cr sorption isotherms (sorbed Cr ( $\text{mmol kg}^{-1}$ ) vs. Cr concentration in the equilibrium solution ( $\mu\text{mol L}^{-1}$ )) fitted to the Freundlich model.

The sorption fitted the Freundlich isotherm in both soils ( $r^2 = 0.822$  for the Vitric Andosol and  $0.976$  for the Silandic Andosol). The fitted equations were  $Q = 1.061 * c^{0.2659}$  for the Vitric Andosol and  $Q = 0.0608 * c^{0.7127}$  for the Silandic Andosol. The constant  $K_F$  was higher in the Vitric Andosol (1.061 vs. 0.0608), while the constant  $m$  was lower in the Vitric Andosol (0.2659 vs. 0.7127).

The Cr desorption in  $\text{NaNO}_3$  was high compared to V and As desorption, and always less than 40% of the adsorbed Cr in both soils (Table 2). The desorption isotherms (Figure 7) also fitted the Freundlich model. The fitted equations were  $Q = 1.215 * c^{0.2351}$ ,  $r^2 = 0.736$  for the Vitric Andosol and  $Q = 0.0408 * c^{0.9249}$ ,  $r^2 = 0.982$  for the Silandic Andosol. The sorption and desorption isotherms were almost coincident in the Vitric Andosol, indicating the reversibility of the sorption. On the contrary, in the Silandic Andosol the desorption isotherm was above the sorption isotherm, indicating that the sorption is irreversible.

The addition of phosphate significantly increased the Cr desorption (Table 2). The sum of chromate released in the two desorption processes was often more than 50% of the previously sorbed chromate. For an initial addition of  $1.9 \text{ mmol Cr L}^{-1}$  ( $38.5 \text{ mmol Cr kg}^{-1}$ ), the residual sorbed Cr (after desorption with phosphate) varied between  $3.1 \text{ mmol kg}^{-1}$  in the Vitric Andosol and  $4.2 \text{ mmol kg}^{-1}$  in the Silandic Andosol.

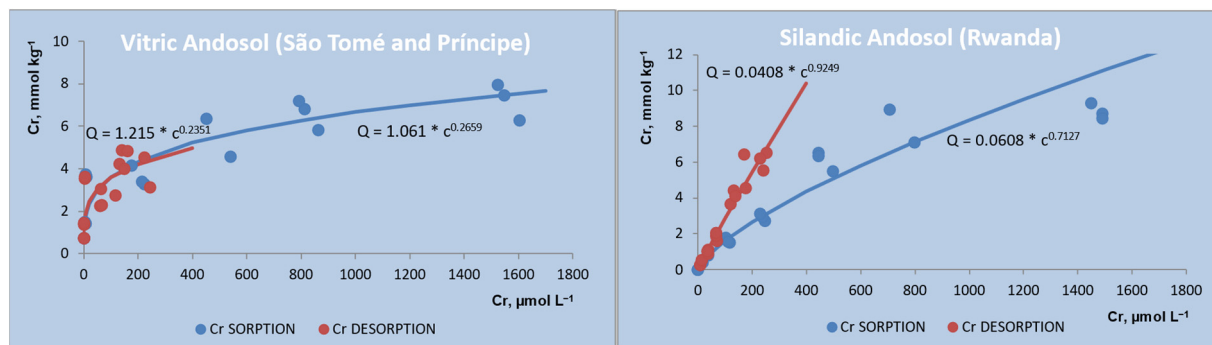


**Figure 7.** Cr sorption and desorption isotherms (sorbed Cr ( $\text{mmol kg}^{-1}$ ) vs. Cr concentration in the equilibrium solution ( $\mu\text{mol L}^{-1}$ )) fitted to the Freundlich model.

#### 4. Discussion

Vanadate and arsenate were intensely sorbed and poorly desorbed by both andosols studied. On the contrary, both soils sorbed relatively low concentrations of chromate, the Silandic Andosol being the one that sorbed more and the Vitric Andosol the one that desorbed more Cr.

Various authors reported a high involvement of Fe and Al compounds in the sorption of soluble forms of vanadium [16,24,26,58,68,69]. Peacock and Sherman [58] showed that V (V) strongly adsorbs onto goethite ( $\alpha\text{-FeOOH}$ ) forming inner-sphere complexes. Gäbler et al. [68], studying vanadium adsorption by thirty German soils, attributed this adsorption mainly to non-crystalline Fe, Mn, and Al oxides and hydroxides. Baken et al. [24] attributed the adsorption of vanadate by four European soils to poorly crystalline oxyhydroxides. Larsson et al. [26] also reported the vanadate sorption by Fe and Al hydrous oxides in 25 European mineral soils; in three out of these 25 soils, K-edge XANES spectroscopy confirmed that the added vanadate had accumulated mostly as adsorbed vanadate on Fe and Al hydrous oxides.

In accordance with the literature, in the present study the strong sorption of vanadate by both andosols suggests that non-crystalline iron and aluminum species, as well as crystalline iron compounds, efficiently sorb vanadate. The vanadate sorption capacity was slightly higher in the Silandic Andosol, richer in non-crystalline iron and aluminum.

The fit to the Freundlich model suggests that the adsorption energy decreases exponentially as the concentration in the adsorbed phase increases. As the amount of adsorbed ions increases, the affinity of the adsorbent surfaces for these ions decreases, since the higher-energy adsorption sites are increasingly occupied; the adsorption energy is progressively lower, varying exponentially with the concentration in the adsorbed phase. As in the present study, V adsorption by 30 German soils [68] and 25 European mineral soils [26] fitted to the Freundlich model. The constant  $K_F$ , slightly higher in the Silandic Andosol (5.495 vs. 4.954), is related by some authors to the sorption capacity, but, according to Russell and Prescott [70], it is related to the retention force of the adsorbate by the adsorbent. The constant  $m$ , related to the accessibility of the sorbing surfaces [71], was very similar in both soils (0.4596 and 0.4468), indicating a rather high heterogeneity of the sorbing surfaces [67].

The hysteresis observed in the vanadate sorption/desorption (Figure 3) indicates the irreversibility of the sorption process. Consistent with our results, Mikkonen and Tummavuori [72] reported that only a minor part of the V retained by three Finnish mineral soils could be removed by KCl treatment.

The very-little desorption of vanadate promoted by the addition of phosphate is in accordance with the assertions that vanadate is more strongly bound than phosphate to iron hydrous oxides [16,28,29] or soils [73].

The results show that both soils are extremely effective against vanadium contamination, reducing the risk of V exportation to water bodies or vegetation.

The higher As sorption on the Vitric Andosol, despite its higher pH, indicates the predominant role of crystalline iron oxides in the sorption of arsenate. This fact is coherent with the observation by Jiang et al. [74] that iron extracted by dithionite-citrate exerts the greatest positive influence on the adsorption of arsenate by soils, while other factors, such as aluminum extracted by oxalate or dithionite-citrate and pH, are less important. Behera et al. [75] reported the efficiency of a goethite-rich iron ore in arsenate sorption, showing that it removes nearly 90% of As from a solution containing 0.265 mg As L<sup>-1</sup>. Additionally, Mansfeldt and Overesch [76] highlighted the role of iron oxides in the arsenate adsorption. Similarly, Gustafsson [77] and Pigna et al. [12] reported that arsenate is sorbed more on Fe than Al oxides. Arsenic forms inner-sphere complexes with goethite, ferrihydrite, amorphous Fe hydroxides, and Al oxides [55,78–80]. In addition, short-range ordered aluminosilicates, clays, and manganese oxides can adsorb As in soils [78,80]. Hue [32] attributed As sorption by Hawaiian andosols to amorphous aluminosilicates and iron oxides.

The sorbed As concentrations for the highest concentration in the equilibrating solution (25 mmol As kg<sup>-1</sup> in both soils) were much higher than those reported by Jiang et al. [56] for Chinese agricultural soils, and even higher than the maximum adsorption value predicted by the Langmuir isotherm for those soils. Those Chinese soils had lower concentrations of Fe and Al extractable by oxalate and dithionite-citrate than the soils in the present study. The sorption values in the present study are comparable to those reported by Smith et al. [81] for the surface horizon of an Oxisol from Australia, which has 16% Fe<sub>d</sub> and 1.6% Al<sub>d</sub> and low concentrations of Fe<sub>o</sub> and Al<sub>o</sub>.

The fit to the Temkin model suggests that the adsorption energy decreases linearly as the concentration in the adsorbed phase increases. The affinity of the adsorbing surfaces for arsenate decreases as the amount of adsorbed arsenate increases, while the higher-energy adsorption sites are increasingly occupied; the adsorption energy is progressively lower, varying linearly with the surface coverage. Unlike our results, Yolcubal and Akyol [82] reported, for calcareous soils of Turkey, that the best fit was to the Freundlich model. Similarly, Smith et al. [81] reported the fit to the Freundlich model in surface horizons of four Australian soils. In the case of the Chinese agricultural soils studied by Jiang et al. [56], the best fit was to the Langmuir model. The fit to the Langmuir isotherm implies a finite number of uniform adsorption sites, with the same sorption energy, and the absence of interactions among the sorbed ions [67]. In the present study, the higher values of the constants A and B, related to the heat of adsorption, in the Vitric Andosol than in the Silandic Andosol indicate a higher affinity for arsenic of active surfaces in the Vitric Andosol.

The Vitric Andosol, having a very high sorption, showed also a very low desorption, less than the Silandic Andosol, confirming the As retention efficiency of crystalline iron oxides.

Sorption/desorption processes control the As concentration in the soil solution and the risk of exportation to vegetation and water bodies [78,80,81]. Both soils studied, particularly the Vitric Andosol, can effectively protect other environmental compartments against arsenic contamination.

Phosphate is known to displace sorbed As from soils [78–80]. Applications of relatively high rates of P fertilizers have been shown to enhance As mobility [30,32]. The higher As desorption with phosphate from the Silandic Andosol than from the Vitric Andosol is in accordance with the finding by Violante and Pigna [83] that iron-rich crystalline minerals were more effective in sorbing arsenate than phosphate, while more phosphate than arsenate was sorbed on non-crystalline and crystalline Al compounds.

The chromate sorption was notably lower than those of vanadate and arsenate. The sorption was higher than that published by Fernandez-Pazos et al. [84] for surface horizons of two Spanish soils with lower concentrations of iron and aluminum extractable by oxalate than those in the present study. The sorption was similar to that reported by Jiang et al. [40] for a subsurface horizon of an Acrisol from southern China, with a lower concentration of Fe<sub>d</sub> than those in the present study, and lower than those of two Ferralsols with a higher

concentration of  $Fe_d$ . According to these authors, iron oxides are major adsorbents for chromate on those Chinese variable-charge soils.

The Cr sorption by the Vitric Andosol was higher than that of the Silandic Andosol at low concentrations in solution, while at high concentrations in solution, the Silandic Andosol adsorbed more. The Vitric Andosol seems to have a limited number of adsorption positions with notable affinity for chromate, while the Silandic Andosol must have a higher number of adsorption sites but with lower chromate affinity. In contrast to sorption, at low concentrations in solution the desorption was low in the Vitric Andosol and higher in the Silandic Andosol; at high concentrations in solution, the desorption was higher in the Vitric Andosol than in the Silandic Andosol. The Vitric Andosol could be more efficient than the Silandic Andosol as a protector of the environment in the case of slight chromium contamination, while the opposite would be true in the case of heavy contamination.

The fit to the Freundlich model suggests that the adsorption energy decreases exponentially as the concentration in the adsorbed phase increases. Fernandez-Pazos et al. [84] also reported the fit to Freundlich model for surface horizons of two Spanish soils. The higher constant  $K_F$  and the lower constant  $m$  in the Vitric Andosol indicates that it retains the chromate more strongly, but its sorbing surfaces have a high heterogeneity and are less accessible to the sorbate. Values of  $m$  close to 1, as in the Silandic Andosol, indicate a low heterogeneity and a high accessibility of the sorbent surfaces [67,71].

According to Fendorf [37], chromate can form inner-sphere complexes (specific adsorption) with goethite and, presumably, also with hydrous aluminum oxides. According to Jiang et al. [40], both specific adsorption and electrostatic adsorption contribute to chromate adsorption by variable-charge soils (Ferralsols, Acrisol). Saeki [85] reported that chromate is adsorbed by a Silandic Andosol forming outer-sphere complex.

The low sorption and high desorption of chromate indicate a low efficiency of both soils as chromate sorbents and a high risk of mobility of this anion to the environment. Nevertheless, the Vitric Andosol effectively retains small amounts of chromium. The higher value of  $m$  in the Freundlich equation and the irreversibility of chromate sorption by the Silandic Andosol seems to indicate the major role of non-crystalline Al and Fe oxides in chromate sorption.

The additional desorption with phosphate was less than that produced with  $NaNO_3$ . Additionally, in this desorption, the Cr released from the Vitric Andosol was very low for initial additions up to  $10 \text{ mg Cr L}^{-1}$  ( $0.19 \text{ mmol L}^{-1}$ ). The sum of chromate released in the two desorption processes reached over 50% in both soils (Table 2). This desorption is in accordance with the higher affinity of phosphate for iron oxides and soil surfaces compared with chromate [41,85].

According to Fendorf et al. [86], the potential hazard posed by Cr(VI) can be prevented by reducing it to Cr(III), using materials such as Fe(II), sulfides, and organic compounds, or by biological (i.e., enzymatic) reduction. This could be an alternative to the weak Cr(VI) sorption by soils.

## 5. Conclusions

Both the Silandic Andosol of Rwanda and the Vitric Andosol of São Tomé showed high sorption and low desorption of vanadate and arsenate, while for chromate the sorption was relatively low and the desorption relatively high. The V sorption was very similar in both andosols, indicating that non-crystalline iron and aluminum species, as well as crystalline iron compounds, efficiently sorb vanadate. The higher As sorption in the Vitric Andosol, rich in crystalline iron oxides, along with the very low desorption, highlight the role of these compounds in arsenate sorption. Chromium was more sorbed by the Vitric Andosol at low concentrations and by the Silandic Andosol at high concentrations, indicating a stronger interaction between sorbent and sorbate, but lower sorption capacity in the Vitric Andosol.

The V and Cr sorption and desorption isotherms fitted to the Freundlich model, while the As isotherms conformed to the Temkin model. Hysteresis was observed for V sorption/desorption in both soils and for Cr sorption/desorption in the Silandic Andosol.

Phosphate hardly displaced sorbed vanadate and induced a moderate desorption of arsenate, particularly from the Silandic Andosol. Conversely, phosphate increased the chromate desorption from both andosols up to values over 50% of the sorbed chromate. The phosphate fertilization could increase the environmental risk in the cases of soil contamination by arsenate or chromate.

Both andosols studied can effectively protect other environmental compartments (vegetation, water bodies) against contamination by vanadium and arsenic. However, the relatively weak sorption of chromate reveals the low efficiency of sorption by soils as a means to combat chromium pollution. In this case, the reduction and immobilization as chromium (III) could be an alternative to the adsorption by soil components as a remediation method for contaminated soils. The reduction of Cr(VI) can be accomplished by the addition of easily oxidizable organic matter.

**Author Contributions:** Conceptualization: M.L.F.-M.; methodology: M.L.F.-M.; investigation: M.L.F.-M. and S.G.-R.; resources: M.L.F.-M.; data curation: M.L.F.-M. and S.G.-R.; writing—original draft preparation: M.L.F.-M.; writing—review and editing: M.L.F.-M.; supervision: M.L.F.-M.; funding acquisition: M.L.F.-M. Both authors have read and agreed to the published version of the manuscript.

**Funding:** This research received no external funding.

**Institutional Review Board Statement:** Not applicable.

**Informed Consent Statement:** Not applicable.

**Data Availability Statement:** The data presented in this study are available in article.

**Conflicts of Interest:** The authors declare no conflict of interest.

## References

1. Adegoke, H.I.; Adekola, F.A.; Fatoki, O.S.; Ximba, B.J. Sorptive Interaction of Oxyanions with Iron Oxides: A Review. *Pol. J. Environ. Stud.* **2013**, *22*, 7–24.
2. Bastounopoulou, M.; Gasparatos, D.; Haidouti, C.; Massas, I. Chemical Fractionation and Sorption of Phosphorus in Greek Inceptisols. *J. Agric. Sci. Technol. A* **2011**, *1*, 33–38. [[CrossRef](#)]
3. Jiang, X.; Peng, C.; Fu, D.; Chen, Z.; Shen, L.; Li, Q.; Ouyang, T.; Wang, Y. Removal of arsenate by ferrihydrite via surface complexation and surface precipitation. *Appl. Surf. Sci.* **2015**, *353*, 1087–1094. [[CrossRef](#)]
4. Jiang, Y.; Yin, X.; Luo, X.; Yu, L.; Sun, H.; Wang, N.; Mathews, S. Sorption of vanadium (V) on three typical agricultural soil of the Loess Plateau, China. *Environ. Pollut. Bioavailab.* **2019**, *31*, 120–130. [[CrossRef](#)]
5. Kumar, E.; Bhatnagar, A.; Hogland, W.; Marques, M.; Sillanpaa, M. Interaction of inorganic anions with iron-mineral adsorbents in aqueous media—A review. *Adv. Colloid Interface Sci.* **2014**, *203*, 11–21. [[CrossRef](#)] [[PubMed](#)]
6. Kumar, E.; Bhatnagar, A.; Hogland, W.; Marques, M.; Sillanpaa, M. Interaction of anionic pollutants with Al-based adsorbents in aqueous media—A review. *Chem. Eng. J.* **2014**, *241*, 443–456. [[CrossRef](#)]
7. Kumar, R.; Kumar, R.; Mittal, S.; Arora, M.; Babu, J.N. Role of soil physicochemical characteristics on the present state of arsenic and its adsorption in alluvial soils of two agri-intensive region of Bathinda, Punjab, India. *J. Soils Sediments* **2016**, *16*, 605–620. [[CrossRef](#)]
8. Parfitt, R.L. Anion adsorption by soils and soil materials. In *Advances in Agronomy*; Brady, N.C., Ed.; Academic Press: Cambridge, MA, USA, 1979; Volume 30, pp. 1–50.
9. Singh, B.R.; Krogstad, T.; Shivay, Y.S.; Shivakumar, B.G.; Bakkegard, M. Phosphorus fractionation and sorption in P-enriched soils of Norway. *Nutr. Cycl. Agroecosyst.* **2005**, *73*, 245–256. [[CrossRef](#)]
10. Wendling, L.A.; Blomberg, P.; Sarlin, T.; Priha, O.; Arnold, M. Phosphorus sorption and recovery using mineral-based materials: Sorption mechanisms and potential phytoavailability. *Appl. Geochem.* **2013**, *37*, 157–169. [[CrossRef](#)]
11. Sparks, D.L. Metal and oxyanion sorption on naturally occurring oxide and clay mineral surfaces. In *Environmental Catalysis*; Grassian, V.H., Ed.; CRC Press LLC: Boca Raton, FL, USA, 2005; pp. 3–36.
12. Pigna, M.; Caporale, A.G.; Cavalca, L.; Sommella, A.; Violante, A. Arsenic in the Soil Environment: Mobility and Phytoavailability. *Environ. Eng. Sci.* **2015**, *32*, 551–563. [[CrossRef](#)]
13. Schlesinger, W.H.; Klein, E.M.; Vengosh, A. Global biogeochemical cycle of vanadium. *Proc. Natl. Acad. Sci. USA* **2017**, *114*, E11092–E11100. [[CrossRef](#)] [[PubMed](#)]



14. Imtiaz, M.; Rizwan, M.S.; Xiong, S.; Li, H.; Ashraf, M.; Shahzad, S.M.; Shahzad, M.; Rizwan, M.; Tu, S. Vanadium, recent advancements and research prospects: A review. *Environ. Int.* **2015**, *80*, 79–88. [CrossRef]
15. Watt, J.A.J.; Burke, I.T.; Edwards, R.A.; Malcolm, H.M.; Mayes, W.M.; Olszewska, J.P.; Pan, G.; Graham, M.C.; Heal, K.V.; Rose, N.L.; et al. Vanadium: A Re-Emerging Environmental Hazard. *Environ. Sci. Technol.* **2018**, *52*, 11973–11974. [CrossRef] [PubMed]
16. Gustafsson, J.P. Vanadium geochemistry in the biogeosphere—speciation, solid-solution interactions, and ecotoxicity. *Appl. Geochem.* **2019**, *102*, 1–25. [CrossRef]
17. Kabata-Pendias, A. *Trace Elements in Soils and Plants*; CRC Press: Boca Raton, FL, USA, 2011.
18. Larsson, M.A.; Baken, S.; Gustafsson, J.P.; Hadialhejazi, G.; Smolders, E. Vanadium bioavailability and toxicity to soil microorganisms and plants. *Environ. Toxicol. Chem.* **2013**, *32*, 2266–2273. [CrossRef] [PubMed]
19. Rattner, B.A.; McKernan, M.A.; Eisenreich, K.M.; Link, W.A.; Olsen, G.H.; Hoffman, D.J.; Knowles, K.A.; McGowan, P.C. Toxicity and hazard of vanadium to Mallard ducks (*Anas platyrhynchos*) and Canada geese (*Branta canadensis*). *J. Toxicol. Environ. Health Part A Curr. Issues* **2006**, *69*, 331–351. [CrossRef] [PubMed]
20. Rowe, C.L.; Heyes, A.; Hopkins, W. Effects of dietary vanadium on growth and lipid storage in a larval anuran: Results from studies employing ad libitum and rationed feeding. *Aquat. Toxicol.* **2009**, *91*, 179–186. [CrossRef]
21. Shaheen, S.M.; Alessi, D.S.; Tack, F.M.G.; Ok, Y.S.; Kim, K.-H.; Gustafsson, J.P.; Sparks, D.L.; Rinklebe, J. Redox chemistry of vanadium in soils and sediments: Interactions with colloidal materials, mobilization, speciation, and relevant environmental implications—A review. *Adv. Colloid Interface Sci.* **2019**, *265*, 1–13. [CrossRef] [PubMed]
22. Vessey, C.J.; Schmidt, M.P.; Abdollahzhad, M.; Peak, D.; Lindsay, M.B.J. Adsorption of (Poly)vanadate onto Ferrihydrite and Hematite: An In Situ ATR–FTIR Study. *ACS Earth Space Chem.* **2020**, *4*, 641–649. [CrossRef]
23. United States Environmental Protection Agency. Contaminant Candidate List (CCL) and Regulatory Determination: Chemical Contaminants—CCL 4. Available online: <https://www.epa.gov/ccl/chemical-contaminants-ccl-4> (accessed on 27 June 2020).
24. Baken, S.; Larsson, M.A.; Gustafsson, J.P.; Cubadda, F.; Smolders, E. Ageing of vanadium in soils and consequences for bioavailability. *Eur. J. Soil Sci.* **2012**, *63*, 839–847. [CrossRef]
25. Moreno-Alvarez, J.M.; Orellana-Gallego, R.; Fernandez-Marcos, M.L. Potentially Toxic Elements in Urban Soils of Havana, Cuba. *Environments* **2020**, *7*, 43. [CrossRef]
26. Larsson, M.A.; Hadialhejazi, G.; Gustafsson, J.P. Vanadium sorption by mineral soils: Development of a predictive model. *Chemosphere* **2017**, *168*, 925–932. [CrossRef] [PubMed]
27. Huang, J.-H.; Huang, F.; Evans, L.; Glasauer, S. Vanadium: Global (bio)geochemistry. *Chem. Geol.* **2015**, *417*, 68–89. [CrossRef]
28. Blackmore, D.P.T.; Ellis, J.; Riley, P.J. Treatment of a vanadium-containing effluent by adsorption/coprecipitation with iron oxyhydroxide. *Water Res.* **1996**, *30*, 2512–2516. [CrossRef]
29. Larsson, M.A.; Persson, I.; Sjöstedt, C.; Gustafsson, J.P. Vanadate complexation to ferrihydrite: X-ray absorption spectroscopy and CD-MUSIC modelling. *Environ. Chem.* **2017**, *14*, 141–150. [CrossRef]
30. Violante, A.; Gaudio, S.D.; Pigna, M.; Pucci, M.; Amalfitano, C. Sorption and desorption of arsenic by soil minerals and soils in the presence of nutrients and organics. In *Soil Mineral Microbe–Organic Interactions: Theories and Applications*; Springer: Berlin/Heidelberg, Germany, 2008; pp. 39–69. [CrossRef]
31. Mandal, B.K.; Suzuki, K.T. Arsenic round the world: A review. *Talanta* **2002**, *58*, 201–235. [CrossRef]
32. Hue, N.V. Arsenic chemistry and remediation in Hawaiian soils. *Int. J. Phytoremediat.* **2013**, *15*, 105–116. [CrossRef]
33. Biasioli, M.; Grcman, H.; Kralj, T.; Madrid, F.; Diaz-Barrientos, E.; Ajmone-Marsan, E. Potentially toxic elements contamination in urban soils: A comparison of three European cities. *J. Environ. Qual.* **2007**, *36*, 70–79. [CrossRef]
34. Madrid, F.; Biasioli, M.; Ajmone-Marsan, F. Availability and bioaccessibility of metals in fine particles of some urban soils. *Arch. Environ. Contam. Toxicol.* **2008**, *55*, 21–32. [CrossRef]
35. Franco-Uria, A.; Lopez-Mateo, C.; Roca, E.; Fernandez-Marcos, M.L. Source identification of heavy metals in pastureland by multivariate analysis in NW Spain. *J. Hazard. Mater.* **2009**, *165*, 1008–1015. [CrossRef]
36. Taylor, R.W.; Shen, S.Y.; Blean, W.F.; Tu, S.I. Chromate removal by dithionite-reduced clays: Evidence from direct X-ray adsorption near edge spectroscopy (XANES) of chromate reduction at clay surfaces. *Clays Clay Miner.* **2000**, *48*, 648–654. [CrossRef]
37. Fendorf, S.E. Surface-reactions of chromium in soils and waters. *Geoderma* **1995**, *67*, 55–71. [CrossRef]
38. Mishra, S.; Bharagava, R.N. Toxic and genotoxic effects of hexavalent chromium in environment and its bioremediation strategies. *J. Environ. Sci. Health Part C* **2016**, *34*, 1–32. [CrossRef]
39. Eick, M.J.; Peak, J.D.; Brady, W.D. The effect of oxyanions on the oxalate-promoted dissolution of goethite. *Soil Sci. Soc. Am. J.* **1999**, *63*, 1133–1141. [CrossRef]
40. Jiang, J.; Xu, R.K.; Wang, Y.; Zhao, A.Z. The mechanism of chromate sorption by three variable charge soils. *Chemosphere* **2008**, *71*, 1469–1475. [CrossRef]
41. Perez, C.; Antelo, J.; Fiol, S.; Arce, F. Modeling oxyanion adsorption on ferrallic soil, part 2: Chromate, selenate, molybdate, and arsenate adsorption. *Environ. Toxicol. Chem.* **2014**, *33*, 2217–2224. [CrossRef]
42. Neall, V.E. Volcanic soils. In *Land Use, Land Cover and Soil Sciences*; Verheye, W.H., Ed.; EOLSS Publishers: Oxford, UK, 2009; Volume VII, pp. 23–45.
43. Nanzyo, M. Unique properties of volcanic ash soils. *Glob. Environ. Res.* **2002**, *6*, 99–112.
44. Pohl, W.L.; Biryabarema, M.; Lehmann, B. Early Neoproterozoic rare metal (Sn, Ta, W) and gold metallogeny of the Central Africa Region: A review. *Appl. Earth Sci.* **2013**, *122*, 66–82. [CrossRef]



45. Haidula, A.F.; Ellmies, R.; Kayumba, F. *Environmental Monitoring of Small-Scale Mining Areas in Rwanda*; Rwanda Environment Management Authority: Windhoek, Namibia; Kigali, Rwanda, 2011; p. 26.
46. Goldmann, S.; Melcher, F.; Gaebler, H.-E.; Dewaele, S.; De Clercq, F.; Muchez, P. Mineralogy and trace element chemistry of ferberite/reinite from tungsten deposits in central Rwanda. *Minerals* **2013**, *3*, 121–144. [[CrossRef](#)]
47. Nieder, R.; Weber, T.K.D.; Paulmann, I.; Muwanga, A.; Owor, M.; Naramabuye, F.X.; Gakwerere, F.; Biryabarema, M.; Biester, H.; Pohl, W. The geochemical signature of rare-metal pegmatites in the Central Africa Region: Soils, plants, water and stream sediments in the Gatumba tin-tantalum mining district, Rwanda. *J. Geochem. Explor.* **2014**, *144*, 539–551. [[CrossRef](#)]
48. Marcelot, G.; Dupuy, C.; Dostal, J.; Rancon, J.P.; Pouclet, A. Geochemistry of mafic volcanic rocks from the Lake Kivu (Zaire and Rwanda) section of the western branch of the African Rift. *J. Volcanol. Geotherm. Res.* **1989**, *39*, 73–88. [[CrossRef](#)]
49. Rogers, N.W.; James, D.; Kelley, S.P.; De Mulder, M. The generation of potassic lavas from the Eastern Virunga province, Rwanda. *J. Petrol.* **1998**, *39*, 1223–1247. [[CrossRef](#)]
50. Flügge, J.; Muwanga, A.; Trümper, K.; Zachmann, D.; Pohl, W. Exploratory geochemical assessment of stream water and sediment contamination in Gatumba tin and tantalum mining district, Rwanda. *Zentralblatt für Geol. und Paläontologie* **2007**, *233*, 246.
51. Belay, I.G.; Tanaka, R.; Kitagawa, H.; Kobayashi, K.; Nakamura, E. Origin of ocean island basalts in the West African passive margin without mantle plume involvement. *Nat. Commun.* **2019**, *10*. [[CrossRef](#)]
52. Fitton, J.G.; Dunlop, H.M. The Cameroon Line, West-Africa, and its bearing on the origin of oceanic and continental alkali basalt. *Earth Planet. Sci. Lett.* **1985**, *72*, 23–38. [[CrossRef](#)]
53. IUSS Working Group WRB. *World Reference Base for Soil Resources 2014, Update 2015: International Soil Classification System for Naming Soils and Creating Legends for Soil Maps*; FAO: Rome, Italy, 2015; Volume 106.
54. Fendorf, S.; Eick, M.J.; Grossl, P.; Sparks, D.L. Arsenate and chromate retention mechanisms on goethite: 1. Surface structure. *Environ. Sci. Technol.* **1997**, *31*, 315–320. [[CrossRef](#)]
55. Goldberg, S.; Johnston, C.T. Mechanisms of arsenic adsorption on amorphous oxides evaluated using macroscopic measurements, vibrational spectroscopy, and surface complexation modeling. *J. Colloid Interface Sci.* **2001**, *234*, 204–216. [[CrossRef](#)]
56. Jiang, W.; Zhang, S.Z.; Shan, X.Q.; Feng, M.H.; Zhu, Y.G.; McLaren, R.G. Adsorption of arsenate on soils: Part 1: Laboratory batch experiments using 16 Chinese soils with different physiochemical properties. *Environ. Pollut.* **2005**, *138*, 278–284. [[CrossRef](#)]
57. Johnston, C.P.; Chrysochoou, M. Mechanisms of Chromate, Selenate, and Sulfate Adsorption on Al-Substituted Ferrihydrite: Implications for Ferrihydrite Surface Structure and Reactivity. *Environ. Sci. Technol.* **2016**, *50*, 3589–3596. [[CrossRef](#)]
58. Peacock, C.L.; Sherman, D.M. Vanadium(V) adsorption onto goethite ( $\alpha$ -FeOOH) at pH 1.5 to 12: A surface complexation model based on ab initio molecular geometries and EXAFS spectroscopy. *Geochim. Cosmochim. Acta* **2004**, *68*, 1723–1733. [[CrossRef](#)]
59. García-Rodeja, E.; Nóvoa, J.C.; Pontevedra, X.; Martínez-Cortizas, A.; Buurman, P. Aluminium and iron fractionation of European volcanic soils by selective dissolution techniques. In *Soils of Volcanic Regions in Europe*; Arnalds, Ó., Óskarsson, H., Bartoli, F., Buurman, P., Stoops, G., García-Rodeja, E., Eds.; Springer: Berlin/Heidelberg, Germany, 2007; pp. 325–351. [[CrossRef](#)]
60. Parfitt, R.L.; Childs, C.W. Estimation of forms of Fe and Al—A review, and analysis of contrasting soils by dissolution and Mossbauer methods. *Soil Res.* **1988**, *26*, 121–144. [[CrossRef](#)]
61. Sanchez, P.A.; Palm, C.A.; Buol, S.W. Fertility capability soil classification: A tool to help assess soil quality in the tropics. *Geoderma* **2003**, *114*, 157–185. [[CrossRef](#)]
62. Blakemore, L.C. *Acid Oxalate-Extractable Iron, Aluminium and Silicon*; ICOMAND: Washington, DC, USA, 1983.
63. Holmgren, G.G. A rapid citrate-dithionite extractable iron procedure. *Soil Sci. Soc. Am. Proc.* **1967**, *31*, 210–211. [[CrossRef](#)]
64. Gonzalez-Rodriguez, S.; Fernandez-Marcos, M.L. Phosphate sorption and desorption by two contrasting volcanic soils of equatorial Africa. *PeerJ* **2018**, *6*, e5820. [[CrossRef](#)] [[PubMed](#)]
65. Lin, Z.; Puls, R.W. Adsorption, desorption and oxidation of arsenic affected by clay minerals and aging process. *Environ. Geol.* **2000**, *39*, 753–759. [[CrossRef](#)]
66. Mead, J.A. A comparison of the Langmuir, Freundlich and Temkin equations to describe phosphate adsorption properties of soils. *Aust. J. Soil Res.* **1981**, *19*, 333–342. [[CrossRef](#)]
67. Goldberg, S. Equations and models describing adsorption processes in soils. In *Chemical Processes in Soils*; Tabatabai, M.A., Sparks, D.L., Eds.; Soil Science Society of America: Madison, WI, USA, 2005; pp. 489–517. [[CrossRef](#)]
68. Gäbler, H.E.; Glüh, K.; Bahr, A.; Utermann, J. Quantification of vanadium adsorption by German soils. *J. Geochem. Explor.* **2009**, *103*, 37–44. [[CrossRef](#)]
69. Naeem, A.; Westerhoff, P.; Mustafa, S. Vanadium removal by metal (hydr)oxide adsorbents. *Water Res.* **2007**, *41*, 1596–1602. [[CrossRef](#)]
70. Russell, E.J.; Prescott, J.A. The reaction between dilute acids and the phosphorus compounds of the soil. *J. Agric. Sci.* **1916**, *8*, 65–110. [[CrossRef](#)]
71. Skopp, J. Derivation of the Freundlich Adsorption Isotherm from Kinetics. *J. Chem. Educ.* **2009**, *86*, 1341. [[CrossRef](#)]
72. Mikkonen, A.; Tummavuori, J. Retention of vanadium (V) by three Finnish mineral soils. *Eur. J. Soil Sci.* **1994**, *45*, 361–368. [[CrossRef](#)]
73. Sun, W.; Li, X.; Padilla, J.; Elbana, T.A.; Selim, H.M. The Influence of Phosphate on the Adsorption-Desorption Kinetics of Vanadium in an Acidic Soil. *J. Environ. Qual.* **2019**, *48*, 686–693. [[CrossRef](#)]
74. Jiang, W.; Zhang, S.Z.; Shan, X.Q.; Feng, M.H.; Zhu, Y.G.; McLaren, R.G. Adsorption of arsenate on soils: Part 2: Modeling the relationship between adsorption capacity and soil physiochemical properties using 16 Chinese soils. *Environ. Pollut.* **2005**, *138*, 285–289. [[CrossRef](#)] [[PubMed](#)]

75. Behera, R.K.; Rout, K.; Nayak, B.; Das, N.N. Removal of selenium and arsenic oxyanions using natural goethite-rich iron ore from Daitari, Orissa, India: Effect of heat treatment. *Adsorpt. Sci. Technol.* **2012**, *30*, 867–879. [[CrossRef](#)]
76. Mansfeldt, T.; Overesch, M. Arsenic Mobility and Speciation in a Gleysol with Petrogleyic Properties: A Field and Laboratory Approach. *J. Environ. Qual.* **2013**, *42*, 1130–1141. [[CrossRef](#)] [[PubMed](#)]
77. Gustafsson, J.P. Modelling competitive anion adsorption on oxide minerals and an allophane-containing soil. *Eur. J. Soil Sci.* **2001**, *52*, 639–653. [[CrossRef](#)]
78. Smith, E.; Naidu, R.; Alston, A.M. Arsenic in the soil environment: A review. In *Advances in Agronomy*; Donald, L.S., Ed.; Academic Press: Cambridge, MA, USA, 1998; Volume 64, pp. 149–195.
79. Moreno-Jiménez, E.; Esteban, E.; Peñalosa, J. The fate of arsenic in soil-plant systems. In *Reviews of Environmental Contamination and Toxicology*; Whitacre, D.M., Ed.; Springer: New York, NY, USA, 2012; Volume 215, pp. 1–37.
80. Campbell, K.M.; Nordstrom, D.K. Arsenic Speciation and Sorption in Natural Environments. *Rev. Mineral. Geochem.* **2014**, *79*, 185–216. [[CrossRef](#)]
81. Smith, E.; Naidu, R.; Alston, A.M. Chemistry of inorganic arsenic in soils: II. Effect of phosphorus, sodium, and calcium on arsenic sorption. *J. Environ. Qual.* **2002**, *31*, 557–563. [[CrossRef](#)]
82. Yolcubal, I.; Akyol, N.H. Adsorption and transport of arsenate in carbonate-rich soils: Coupled effects of nonlinear and rate-limited sorption. *Chemosphere* **2008**, *73*, 1300–1307. [[CrossRef](#)]
83. Violante, A.; Pigna, M. Competitive sorption of arsenate and phosphate on different clay minerals and soils. *Soil Sci. Soc. Am. J.* **2002**, *66*, 1788–1796. [[CrossRef](#)]
84. Fernández-Pazos, M.T.; Garrido-Rodríguez, B.; Nóvoa-Muñoz, J.C.; Arias-Estévez, M.; Fernández-Sanjurjo, M.J.; Núñez-Delgado, A.; Álvarez, E. Cr(VI) Adsorption and Desorption on Soils and Biosorbents. *Water Air Soil Pollut.* **2012**, *224*, 1366. [[CrossRef](#)]
85. Saeki, K. Adsorption sequence of toxic inorganic anions on a soil. *Bull. Environ. Contam. Toxicol.* **2008**, *81*, 508–512. [[CrossRef](#)] [[PubMed](#)]
86. Fendorf, S.; Wielinga, B.W.; Hansel, C.M. Chromium Transformations in Natural Environments: The Role of Biological and Abiological Processes in Chromium(VI) Reduction. *Int. Geol. Rev.* **2010**, *42*, 691–701. [[CrossRef](#)]